ARTICLES
PUBLISHED ONLINE: 6 APRIL 2014 | DOI: 10.1038/NPHYS2927
nature physics

Parity–time-symmetric whispering-gallery microcavities

Bo Peng[1†], Şahin Kaya Özdemir[1*†], Fuchuan Lei[1,2], Faraz Monifi[1], Mariagiovanna Gianfreda[3,4], Gui Lu Long[2,5], Shanhui Fan[6], Franco Nori[7,8], Carl M. Bender[3] and Lan Yang[1*]

Optical systems combining balanced loss and gain provide a unique platform to implement classical analogues of quantum systems described by non-Hermitian parity–time (PT)-symmetric Hamiltonians. Such systems can be used to create synthetic materials with properties that cannot be attained in materials having only loss or only gain. Here we report PT-symmetry breaking in coupled optical resonators. We observed non-reciprocity in the PT-symmetry-breaking phase due to strong field localization, which significantly enhances nonlinearity. In the linear regime, light transmission is reciprocal regardless of whether the symmetry is broken or unbroken. We show that in one direction there is a complete absence of resonance peaks whereas in the other direction the transmission is resonantly enhanced, a feature directly associated with the use of resonant structures. Our results could lead to a new generation of synthetic optical systems enabling on-chip manipulation and control of light propagation.

Parity–time (PT)-symmetric quantum Hamiltonian systems have attracted increasing attention since it was shown that the eigenvalues of non-Hermitian Hamiltonians $\hat{H}^{\dagger} \neq \hat{H}$ can be entirely real if they respect PT symmetry[1], $PT\hat{H} = \hat{H}PT$. PT-symmetric systems are open physical systems having balanced absorption (loss) and amplification (gain). Remarkably, such systems can exhibit a phase transition[1–3] (spontaneous PT-symmetry breaking) if the parameter controlling the degree of non-Hermiticity exceeds a critical value. Beyond this threshold the eigenvalues become complex even though $PT\hat{H} = \hat{H}PT$ still holds. PT symmetry has been studied experimentally[4–14] and theoretically[15–25] in various physical systems, with optics emerging as the most versatile platform to explore PT-symmetric applications.

So far, experiments in PT-symmetric optics have been limited to waveguides[4–8] in which resonances play no role. Loss-induced transparency[4], power oscillations violating left–right symmetry[5], PT-synthetic photonic lattices[7], and unidirectional invisibility[7,8] have been demonstrated, but other phenomena such as non-reciprocal light transmission[6,15,16,26,27], coexisting coherent perfect absorption and lasing[28–30], photonic analogues of topological insulators[31] and exceptional points in lasers[32] are yet to be realized. These could benefit significantly from resonance structures exhibiting PT symmetry. In particular, optical non-reciprocity[27,33–38] has been a long-sought-after goal in the study of PT symmetry because of its substantial device implications for optical information processing. Here we report PT-symmetry breaking in a system of two directly coupled on-chip optical resonators, and provide direct proof of non-reciprocity in PT-symmetric optics. Our record low power of 1 μW, to observe nonlinearity-induced time-reversal symmetry breaking for non-reciprocal light transmission, could not be achieved without a resonant structure.

Our system consists of two directly coupled microtoroidal whispering-gallery-mode resonators[39,40] (WGMRs), each coupled to a different fibre-taper coupler (Fig. 1a–c). This system is PT symmetric because under parity reflection P the WGMRs become interchanged and under time reversal T loss becomes gain and gain becomes loss. The first microtoroid (μR_1) is an active resonator made from Er^{3+}-doped silica[40–42]; the second microtoroid (μR_2) is a passive (no-gain-medium) resonator made from silica without dopants[40]. Gain in μR_1 was provided in the 1,550 nm wavelength band by optically pumping Er^{3+} ions with a pump laser in the 1,460 nm band. The Q-factors of μR_1 and μR_2 in the 1,550 nm band were 3.3×10^6 and 3×10^7, respectively, and μR_1 had a Q-factor of 2.4×10^6 in the 1,460 nm band (Fig. 1d). The microtoroids were fabricated at the edges of two separate chips placed on nanopositioning systems to control precisely the distance and hence the coupling between the microtoroids (Supplementary Sections A and B1). We mediated the coupling between μR_1 and μR_2 in the 1,550 nm band by controlling the detuning between their resonant wavelengths through the tuning of the resonance wavelength of μR_2 via the thermo-optic effect of silica. There was no coupling between the resonators in the 1,460 nm band; thus, the pump existed only in μR_1. Compensation of the μR_1 losses in the 1,550 nm band with the optical gain provided by Er^{3+} was confirmed by the narrowing of resonance linewidth with increasing pump power (Fig. 1e) and by the emergence of a strong resonance peak (Fig. 1f) due to the amplification of a very weak probe by the gain.

We conducted two sets of experiments using the apparatus in Fig. 1. The first set determined the broken and unbroken PT phases in coupled microcavities with balanced loss and gain as a function of the coupling strength κ, unlike previous experiments where κ was fixed and the gain and loss ratio was varied. We studied the

[1]Department of Electrical and Systems Engineering, Washington University, St Louis, Missouri 63130, USA, [2]State Key Laboratory of Low-dimensional Quantum Physics and Department of Physics, Tsinghua University, Beijing 100084, China, [3]Department of Physics, Washington University, St Louis, Missouri 63130, USA, [4]Dipartimento di Matematica e Fisica Ennio De Giorgi, Universita del Salento and I.N.F.N. Sezione di Lecce, Via Arnesano, I-73100 Lecce, Italy, [5]Tsinghua National Laboratory for Information Science and Technology, Beijing 100084, China, [6]Department of Electrical Engineering, Stanford University, Stanford, California 94305, USA, [7]Center for Emergent Matter Science, RIKEN, Saitama 351-0198, Japan. [8]Physics Department, University of Michigan, Ann Arbor Michigan 48109-1040, USA. [†]These authors contributed equally to this work. *e-mail: yang@ese.wustl.edu; ozdemir@ese.wustl.edu

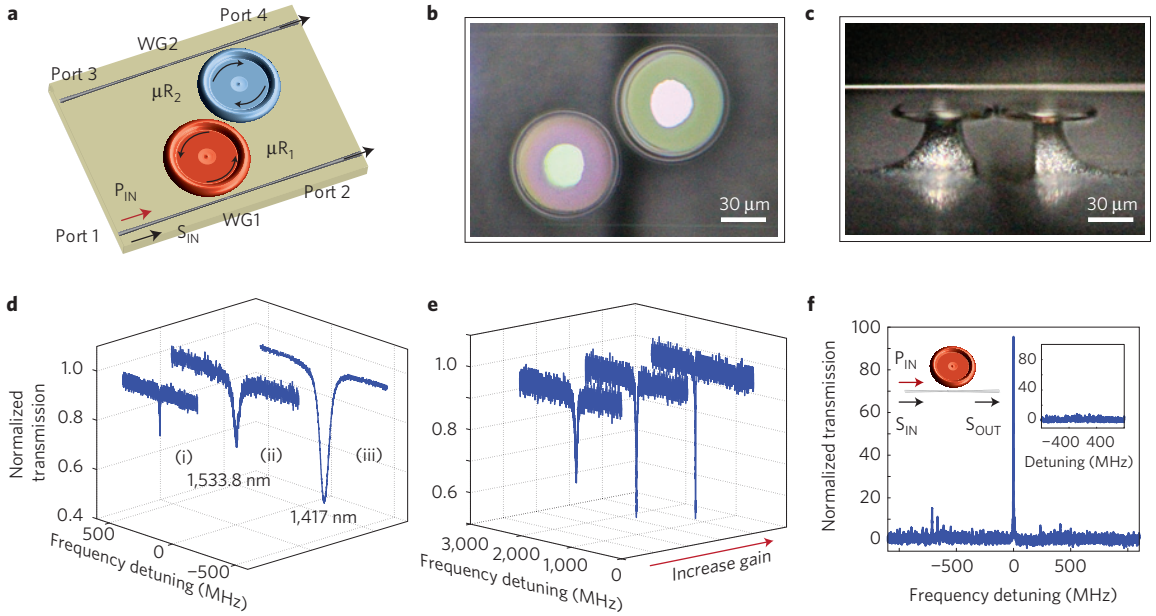

Figure 1 | PT-symmetric whispering-gallery-mode microcavities. a, A system consists of two directly coupled whispering-gallery-mode resonators (WGMRs) and two fibre-taper waveguides. WG1: fibre-taper waveguide with ports 1 and 2. WG2: fibre-taper waveguide with ports 3 and 4. μR_1: active Er^{3+}-doped silica microtoroid. μR_2: passive silica microtoroid. P_{IN}: pump laser in 1,460 nm band to excite Er^{3+} ions that provide gain in 1,550 nm band. S_{IN}: probe light (signal) in 1,550 nm band. **b**,**c**, Top and side views of the coupled resonators. **d**, Transmission spectra showing resonance of μR_2 at 1,533.8 nm (i) and resonances of μR_1 at 1,533.8 nm (ii) and at 1,417.0 nm (iii). **e**, Gain provided by Er^{3+} ions in μR_1 leads to narrower and deeper resonances as pump power (gain) is raised, implying an increasing Q-factor. **f**, Weak probe light is amplified when coupled to μR_1 together with the pump light. Inset shows that without the weak S_{IN} there is no resonance enhancement.

system using only the waveguide (WG1) coupled to μR_1. The pump and the weak probe lasers were input at port 1 and the output transmission spectra were monitored at port 2 in the 1,550 nm band. Without the pump, the coupled-resonator system acted as a passive photonic molecule[43] characterized by two supermodes whose spectral distance increases with increasing κ as seen in Fig. 2a (κ decreases exponentially with increasing distance between μR_1 and μR_2; see Supplementary Fig. 5). This system became PT symmetric when μR_1 was optically pumped to provide gain and μR_2 had a balanced loss. At fixed gain–loss ratio, we monitored the output port as a function of κ and observed the PT phase transition at the threshold coupling strength κ_{PT} (Fig. 2a,b). For $\kappa/\kappa_{PT} < 1$, the system is in a broken-symmetry phase, as seen in both the coalescence of the real parts of the eigenfrequencies (Fig. 2a) and the non-zero difference in their imaginary parts (Fig. 2b). As κ/κ_{PT} approaches 1 from below, the difference in the imaginary parts of the eigenfrequencies decreases and their real parts bifurcate (mode-splitting).

Next, we chose two different WGMs with Q-factors 2.0×10^7 and 3.0×10^7 in μR_2 and adjusted the pump power so that the loss–gain ratio was nearly balanced. We observed the transition from the broken to unbroken phase occurring at different coupling strengths for modes with different Q, that is, different initial loss (Fig. 2c,d). The PT phase transition occurs at higher κ_{PT} for lower Q-factors.

The PT phase transition can be understood intuitively as follows. If the coupling between the resonators is weak, the energy in the active resonator cannot flow fast enough into the passive resonator to compensate the absorption. Thus, the system cannot be in equilibrium and the eigenfrequencies are complex, implying exponential growth or decay. However, if the coupling strength exceeds a critical value, then the system can attain equilibrium because the energy in the active resonator can flow rapidly enough into the passive one to compensate the dissipation.

In our experiments the frequency bifurcation (splitting) is not in orthogonal directions (Fig. 2) as would be expected for ideal systems with exactly balanced gain and loss. Instead, the bifurcation is smooth and the degree of smoothness (how much the system deviates from the exactly balanced case) depends on the pump power. To understand the origin of this behaviour, we revisited the equations of motion for coupled oscillators, which showed that for unbalanced gain and loss, the eigenfrequencies are never exactly real[44,45]. Instead, there is a region of κ where the difference in imaginary parts is large but the difference in real parts is small (but non-zero), and a second region where the difference in imaginary parts is small but non-zero, and the splitting is large. In practical implementations it is impossible to balance the loss and gain exactly, so the mathematical prediction of a smooth bifurcation is physically realistic and consistent with our experiments (Fig. 2).

A linear static dielectric system, even with gain and loss, cannot have non-reciprocal response[27,33,38]. However, a nonlinear system can exhibit strong non-reciprocity. In our second set of experiments we tested this in our PT-symmetric system (Fig. 1a with transmission from input port 1 (4) to output port 4 (1) defined as the forward $T_{1\to4}$ (backward $T_{4\to1}$)) and demonstrated strong non-reciprocal light transmission associated with nonlinearity enhancement induced by PT-symmetry breaking.

We first monitored the output spectra at port 1 as the power of input probe at port 4 was varied while the system was in broken- or unbroken-symmetry phases. A clear nonlinear response was observed in the symmetry-broken phase in contrast to the linear response in the unbroken phase (Fig. 3a). At low power levels where the input–output relation was linear, the system was reciprocal in both the broken- and unbroken-symmetry phases (Fig. 3b,c). Thus, we have direct experimental clarification of reciprocity in PT-symmetric systems; PT symmetry alone is not sufficient for non-reciprocal light transmission. As we increased the input power, the system remained in the linear regime for the unbroken-symmetry phase, whereas the input–output relation became nonlinear in the broken phase (Fig. 3a). These results indicate nonlinearity enhancement (that is, lower threshold for nonlinearity) in the

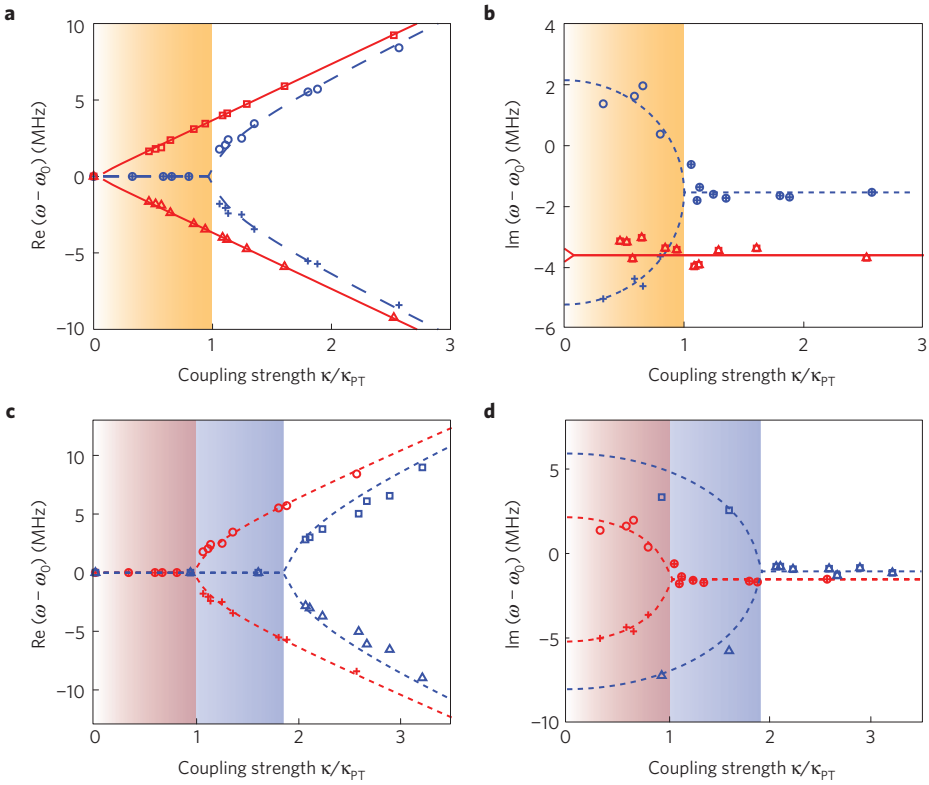

Figure 2 | PT-symmetry breaking in coupled WGM microresonators. a–d, Experimentally obtained real Re(ω) (**a**,**c**) and imaginary Im(ω) (**b**,**d**) parts of the eigenfrequencies of supermodes as a function of coupling κ/κ_{PT} (Supplementary Sections B2 and B3 and Supplementary Fig. 6). ω_0 is the frequency of the resonances before coupling. The data points are obtained from curve-fitting the measured transmission spectra to the analytical model. **a**,**b**, Comparison when resonators are passive (no gain in μR_1: red square and triangular symbols) with Q-factors 2.9×10^7 and 3.0×10^7, respectively, for μR_1 and μR_2, and when one resonator is active and the other is passive (gain in μR_1: blue circular and cross symbols). **c**,**d**, Effect of initial Q-factor (loss) of μR_2 on eigenfrequencies. Two resonances with Q-factors 2.0×10^7 (blue) and 3.0×10^7 (red) are chosen for μR_2. Shaded regions correspond to the broken-PT-symmetric region when gain and loss are balanced. The dashed and solid lines were obtained from the theoretical model using experimentally obtained values of coupling strength, gain and the loss parameters (Supplementary Sections B2–B4 and Figs 5 and 6). The value of κ_{PT} in **c**,**d** is obtained for the case when high $Q = 3.0 \times 10^7$ resonance mode is chosen in μR_2.

broken-symmetry phase, due to the stronger field localization in the resonator with gain, as compared with the unbroken-symmetry phase (Supplementary Section 7 and Fig. 9).

As a result of stronger nonlinearity in the broken-symmetry case, the PT transition is associated with a transition from reciprocal to non-reciprocal behaviour. When the pump at port 1 was OFF (μR_1 and μR_2 are passive) and a weak probe light was input at port 1 or 4, we observed resonance peaks in the forward or backward transmissions (Fig. 4a(i),b(i)) with no resolvable mode splitting. When the pump was set ON and the gain and loss were balanced so as to operate in the unbroken-PT-symmetric region, transmission spectra showed amplified signals with clearly resolved split peaks (Fig. 4a(ii),b(ii)). However, when the coupling strength was decreased so that the system transited into the broken-symmetry region, forward transmission reduced to zero $T_{1\to4} \sim 0$ (Fig. 4a(iii)) but the backward transmission remained high (Fig. 4b(iii)). The transmission spectra showed a single resonance peak, as expected from the theory. Thus, in the broken-symmetry region the input at port 4 was transmitted to port 1 at resonance; however, the input at port 1 could not be transmitted to port 4, in stark contrast with what was observed for the unbroken-symmetry region. This indicates non-reciprocal light transport between ports 1 and 4.

Unlike previous experiments demonstrating non-reciprocal transport in non-PT structures[34–38] and asymmetric behaviour in PT electronics[13], we observed a complete absence of resonance peak in the forward transmission. The advantages of the present design, which brings together PT-symmetric concepts with nonlinearity-induced non-reciprocal light transmission, over the non-PT schemes utilizing nonlinearity are: a significant reduction in the input power to observe non-reciprocity (~1 μW in this work versus 3 W in ref. 34, 0.310 W in ref. 35 and ~85 μW in ref. 37); higher contrast; small footprint; and a complete absence of the signal in one direction but resonantly enhanced transmission in the other direction. This is in stark contrast with other non-reciprocal devices where transmission suffers from high losses (see Supplementary Section B11 for a detailed comparison of this work with other works in the literature). Also, the transmitted signal here was not from spontaneous emission of the gain medium. Without the weak injected signal at input port 4, the output at port 1 was at the noise level, and no resonance peak was observed (inset of Fig. 4b(ii),b(iii)). Resonance enhancement (the peak) was observed only when the weak signal was present (Supplementary Section B8 and Fig. 10). We also observed similar non-reciprocity between ports 2 and 3. These results imply that PT-symmetric WGMRs can have strong non-reciprocal effects (all-optical diode action) in the nonlinear regime with a very low power threshold due to significant enhancement of nonlinearity in the broken-symmetry phase.

Our experiments extend PT-symmetric optics from centimetre/metre-scale structures to on-chip micro-scale structures and, more importantly, from waveguides to microresonators. This overcomes the long-standing open challenge of implementing a true PT-symmetric resonator system in the optical regime and opens the door for exploring new functionalities (for example,

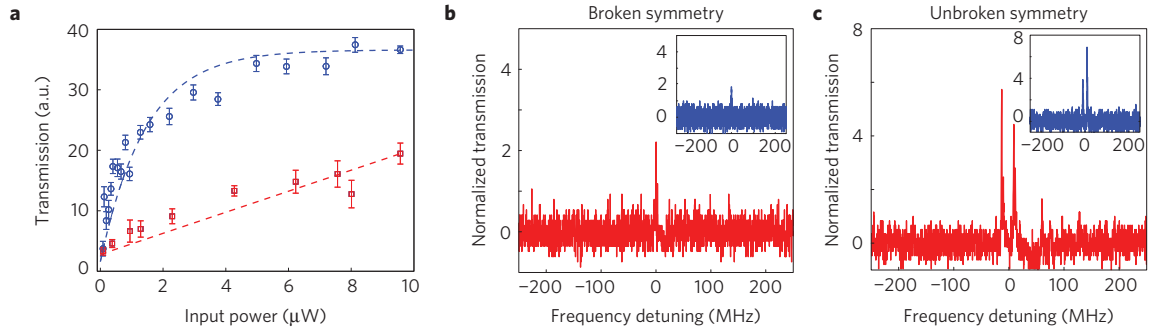

Figure 3 | Input–output relation in PT-symmetric WGMRs and reciprocity in the linear regime. a, Linear input–output relation in the unbroken-symmetry region (red square symbols) but nonlinear in the broken-symmetry region (blue circle symbols). Transmitted signal to port 1 was detected by a photodetector when the input was at port 4. Each data point is the average of ten measurements, and the error bars represent the standard deviations. **b**,**c**, Transmission spectra in the linear regime (input power of ~80 nW) show reciprocal light transmission at forward (blue inset) and backward (red spectra) directions in both the broken- (**b**) and unbroken- (**c**) symmetry regions. The red (blue) spectra were normalized with the signal detected at port 3 (2) when the input was at port 4 (1) and there was no coupling between the fibre tapers and the resonators. The slight difference in the heights of the resonance peaks is attributed to the laser power fluctuations during frequency scanning and to the thermal fluctuations of the environment. These can be minimized, if not completely eliminated, by active stabilization and better control of the experimental conditions (Supplementary Section B10 and Fig. 12).

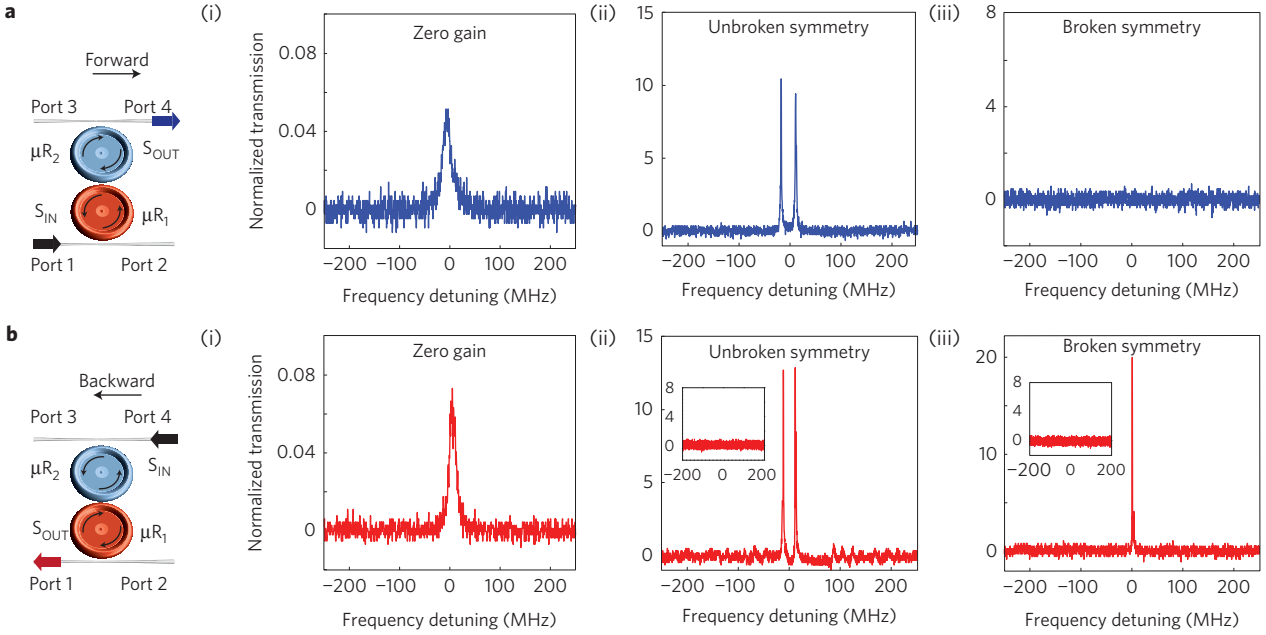

Figure 4 | Experimentally observed unidirectional transmission for PT-symmetric WGM microresonators in the nonlinear regime. a,**b**, When both resonators are passive (zero gain), the transmission is bi-directional (reciprocal), and light is transmitted in both forward (**a**(i)) and backward directions (**b**(i)). In the unbroken-symmetry region, where the coupling exceeds the critical value and gain and loss are balanced, the transmission is still bi-directional (**a**(ii),**b**(ii)). Mode splitting due to coupling is now resolved because gain compensates loss leading to narrower linewidths. In the broken-symmetry region (**a**(iii),**b**(iii)), transmission becomes unidirectional (non-reciprocal). Input in the backward direction reaches the output (**b**(iii)), but input in the forward direction does not (**a**(iii)). This resembles the action of a diode and implies that an all-optical on-chip diode with PT-symmetric WGM microcavities operates in the broken-symmetry region. Inset in (**b**(ii),**b**(iii)) shows the signal at port 1 when there is no input signal at port 4.

coherent-perfect-absorption lasers, topologically protected optical diodes, enhanced nonlinearities and light–matter interactions) that can be achieved only with resonant structures and resonant enhancement. Although we used fibre-taper-coupled microtoroids, our techniques can be extended to other WGMRs and to photonic crystal cavities. Similarly, gain could be provided by quantum dots or other rare-earth ions, and also through nonlinear processes, such as Raman or parametric amplification. Like any non-reciprocal device utilizing resonant effects, our PT-symmetric all-optical diode is bandwidth-limited[36–38]. However, by thermally tuning resonance wavelengths and by using active resonators doped with multiple rare-earth ions, operation over large wavelength bands should be possible. Coupled WGMRs provide a comprehensive framework for understanding resonance effects in PT-symmetric optical systems and could thereby aid in developing on-chip synthetic structures to harness the flow of light. For example, the electromagnetically induced transparency in coupled passive resonators may benefit from PT-symmetric resonators through lossless modulation of the transparency for slowing and stopping of light. Similarly, PT-symmetric microresonators can be used for studying nonlinear Fano resonances that may give rise to ultralow-power and high-contrast switching and non-reciprocity due to their sharp asymmetric line shapes. Moreover, there has been an emerging interest in exploring PT symmetry in various fields,

such as microlasers[42], sensing[46–49], plasmonics[48,50], optomechanics[51] and cavity-quantum electrodynamics[52], where passive WGMRs have been traditionally used. This may bring about new results and physical insights into these fields.

Received 12 September 2013; accepted 19 February 2014; published online 6 April 2014

References

1. Boettcher, S. & Bender, C. M. Real spectra in non-Hermitian Hamiltonians having PT symmetry. *Phys. Rev. Lett.* **80,** 5243–5246 (1998).
2. Bender, C. M. Making sense of non-Hermitian Hamiltonians. *Rep. Prog. Phys.* **70,** 947–1018 (2007).
3. Mostafazadeh, A. Pseudo-Hermiticity versus PT symmetry: the necessary condition for the reality of the spectrum of a non-Hermitian Hamiltonian. *J. Math. Phys.* **43,** 205–214 (2002).
4. Guo, A. *et al.* Observation of PT-symmetry breaking in complex optical potentials. *Phys. Rev. Lett.* **103,** 093902 (2009).
5. Rüter, C. E. *et al.* Observation of parity–time symmetry in optics. *Nature Phys.* **6,** 192–195 (2010).
6. Feng, L. *et al.* Nonreciprocal light propagation in a silicon photonic circuit. *Science* **333,** 729–733 (2011).
7. Regensburger, A. *et al.* Parity–time synthetic photonic lattices. *Nature* **488,** 167–171 (2012).
8. Feng, L. *et al.* Experimental demonstration of a unidirectional reflectionless parity–time metamaterial at optical frequencies. *Nature Mater.* **12,** 108–113 (2012).
9. Schindler, J., Li, A., Zheng, M. C., Ellis, F. M. & Kottos, T. Experimental study of active LRC circuits with PT symmetries. *Phys. Rev. A* **84,** 040101(R) (2011).
10. Zheng, C., Hao, L. & Long, G. L. Observation of fast evolution in parity–time-symmetric system. *Phil. Trans. R. Soc. A* **371,** 20120053 (2013).
11. Bittner, S. *et al.* PT symmetry and spontaneous symmetry breaking in a microwave billiard. *Phys. Rev. Lett.* **108,** 024101 (2012).
12. Bender, C. M., Berntson, B. K., Parker, D. & Samuel, E. Observation of PT phase transition in a simple mechanical system. *Am. J. Phys.* **81,** 173–179 (2013).
13. Bender, N. *et al.* Observation of asymmetric transport in structures with active nonlinearities. *Phys. Rev. Lett.* **110,** 234101 (2013).
14. Chtchelkatchev, N. M., Golubov, A. A., Baturina, T. I. & Vinokur, V. M. Stimulation of the fluctuation superconductivity by PT symmetry. *Phys. Rev. Lett.* **109,** 150405 (2012).
15. Sukhorukov, A. A., Xu, Z. & Kivshar, Y. S. Nonlinear suppression of time reversals in PT-symmetric optical couplers. *Phys. Rev. A* **82,** 043818 (2010).
16. Ramezani, H., Kottos, T., El-Ganainy, R. & Christodoulides, D. N. Unidirectional nonlinear PT-symmetric optical structures. *Phys. Rev. A* **82,** 043803 (2010).
17. Lin, Z. *et al.* Unidirectional invisibility induced by PT-symmetric periodic structures. *Phys. Rev. Lett.* **106,** 213901 (2011).
18. Longhi, S. Invisibility in PT-symmetric complex crystals. *J. Phys. A* **44,** 485302 (2011).
19. Jones, H. F. Analytic results for a PT-symmetric optical structure. *J. Phys. A* **45,** 135306 (2012).
20. Zhu, X., Feng, L., Zhang, P., Yin, X. & Zhang, X. One-way invisible cloak using parity–time symmetric transformation optics. *Opt. Lett.* **38,** 2821–2824 (2013).
21. Hang, C., Huang, G. & Konotop, V. V. PT symmetry with a system of three-level atoms. *Phys. Rev. Lett.* **110,** 083604 (2013).
22. Graefe, E-M. Stationary states of a PT symmetric two-mode Bose-Einstein condensate. *J. Phys. A* **45,** 444015 (2012).
23. Agarwal, G. S. & Qu, K. Spontaneous generation of photons in transmission of quantum fields in PT-symmetric optical systems. *Phys. Rev. A* **85,** 031802 (2012).
24. Benisty, H. *et al.* Implementation of PT symmetric devices using plasmonics: principle and applications. *Opt. Exp.* **19,** 18004 (2011).
25. Lazarides, N. & Tsironis, G. P. Gain-driven discrete breathers in PT-symmetric nonlinear metamaterials. *Phys. Rev. Lett.* **110,** 053901 (2013).
26. Yin, X. & Zhang, X. Unidirectional light propagation at exceptional points. *Nature Mater.* **12,** 175–177 (2013).
27. Fan, S. *et al.* Comment on nonreciprocal light propagation in a silicon photonic circuit. *Science* **335,** 38 (2012).
28. Chong, Y. D., Ge, L., Cao, H. & Stone, A. D. Coherent perfect absorbers: Time-reversed lasers. *Phys. Rev. Lett.* **105,** 053901 (2010).
29. Longhi, S. PT-symmetric laser absorber. *Phys. Rev. A* **82,** 031801(R) (2010).
30. Chong, Y. D., Ge, L. & Stone, A. D. PT-symmetry breaking and laser-absorber modes in optical scattering systems. *Phys. Rev. Lett.* **106,** 093902 (2011).
31. Liang, G. Q. & Chong, Y. D. Optical resonator analog of a two-dimensional topological insulator. *Phys. Rev. Lett.* **110,** 203904 (2013).
32. Liertzer, M. *et al.* Pump-induced exceptional points in lasers. *Phys. Rev. Lett.* **108,** 173901 (2012).
33. Yu, Z. & Fan, S. Complete optical isolation created by indirect interband photonic transitions. *Nature Photon.* **3,** 91–94 (2009).
34. Gallo, K., Assanto, G., Parameswaran, K. R. & Fejer, M. M. All-optical diode in a periodically poled lithium niobate waveguide. *Appl. Phys. Lett.* **79,** 314–316 (2001).
35. Kang, M. S., Butsch, A. & Russell, P. St. J. Reconfigurable light-driven opto-acoustic isolators in photonic crystal fibre. *Nature Photon.* **5,** 549–553 (2011).
36. Bi, L. *et al.* On-chip optical isolation in monolithically integrated non-reciprocal optical resonators. *Nature Photon.* **5,** 758–762 (2011).
37. Fan, L. *et al.* An all-silicon passive optical diode. *Science* **335,** 447–450 (2012).
38. Lira, H., Yu, Z., Fan, S. & Lipson, M. Electrically driven nonreciprocity induced by interband photonic transition on a silicon chip. *Phys. Rev. Lett.* **109,** 033901 (2012).
39. Vahala, K. J. Optical microcavities. *Nature* **106,** 839–846 (2003).
40. Armani, D. K., Kippenberg, T. J., Spillane, S. M. & Vahala, K. J. Ultra-high-*Q* toroid microcavity on a chip. *Nature* **421,** 925–928 (2003).
41. Yang, L., Carmon, T., Min, B., Spillane, S. M. & Vahala, K. J. Erbium-doped and Raman microlasers on a silicon chip fabricated by the sol-gel process. *Appl. Phys. Lett.* **86,** 091114 (2005).
42. He, L., Ozdemir, S. K. & Yang, L. Whispering gallery microcavity lasers. *Laser Photon. Rev.* **7,** 60–82 (2013).
43. Peng, B., Ozdemir, S. K., Zhu, J., Zhu, & Yang, L. Photonic molecules formed by coupled hybrid resonators. *Opt. Lett.* **37,** 3435–3437 (2012).
44. Bender, C. M., Gianfreda, M., Ozdemir, S. K., Peng, B. & Yang, L. Twofold transition in PT-symmetric coupled oscillators. *Phys. Rev. A* **88,** 062111 (2013).
45. Benisty, H., Yan, C., Degiron, A. & Lupu, A. T. Healing near-PT-symmetric structures to restore their characteristic singularities: Analysis and examples. *J. Lightwave Technol.* **30,** 2675–2683 (2012).
46. He, L., Ozdemir, S. K., Zhu, J., Kim, W. & Yang, L. Detecting single viruses and nanoparticles using whispering gallery microlasers. *Nature Nanotech.* **6,** 428–432 (2011).
47. Zhu, J. *et al.* Single nanoparticle detection and sizing by mode-splitting in an ultra-high-*Q* microtoroid resonator. *Nature Photon.* **4,** 46–49 (2010).
48. Dantham, V. R. *et al.* Label-free detection of single protein using a nanoplasmonic-photonic hybrid microcavity. *Nano Lett.* **13,** 3347–3351 (2013).
49. Ozdemir, S. K., Zhu, J., He, L. & Yang, L. Estimation of Purcell factor from mode-splitting spectra in an optical microcavity. *Phys. Rev. A* **83,** 033817 (2011).
50. Bumki, M. *et al.* High-Q surface-plasmon-polariton whispering-gallery microcavity. *Nature* **457,** 455–458 (2009).
51. Kippenberg, T. J. & Vahala, K. J. Cavity optomechanics: Back-action at the mesoscale. *Science* **321,** 1172–1176 (2008).
52. Aoki, T. *et al.* Observation of strong coupling between one atom and a monolithic microresonator. *Nature* **442,** 671–674 (2006).

Acknowledgements

This work is supported by Army Research Office grant No. W911NF-12-1-0026. C.M.B. is supported by US Department of Energy grant No. DE-FG02-91ER40628. F.N. is partially supported by the RIKEN iTHES Project, MURI Center for Dynamic Magneto-Optics, Grant-in-Aid for Scientific Research (S), MEXT Kakenhi on Quantum Cybernetics and the JSPS through its FIRST program. F.L. and G.L.L. are supported by the National Natural Science Foundation of China (Grant Nos 11175094, 91221205), the National Basic Research Program of China (Grant No. 2011CB921602), and the Collaborative Innovation Center of Quantum Matter, Beijing, China.

Author contributions

S.K.O. and L.Y. conceived the idea and designed the experiments; B.P. performed the experiments with help from F.L., F.M. and S.K.O. Theoretical background and simulations were provided by F.L., F.M., M.G., C.M.B., S.F. and F.N. All authors discussed the results, and S.K.O. and L.Y. wrote the manuscript with inputs from all authors. L.Y. supervised the project.

Additional information

Supplementary information is available in the online version of the paper. Reprints and permissions information is available online at www.nature.com/reprints. Correspondence and requests for materials should be addressed to S.K.O. and L.Y.

Competing financial interests

The authors declare no competing financial interests.